Quantum-Chemical Studies of Model Cytochrome P450 Hydrocarbon Oxidation Mechanisms. 1. A MINDO/3 Study of Hydroxylation and Epoxidation Pathways for Methane and Ethylene

Andrew T. Pudzianowski and Gilda H. Loew*

Contribution from the Life Sciences Division, SRI International, Menlo Park, California 94025.
Received December 21, 1979

Abstract: A simple oxene model for cytochrome P450 hydrocarbon hydroxylation and epoxidation, with methane and ethylene as "substrates", has been examined by using the semiempirical MINDO/3 molecular orbital method, in conjunction with rigorous analytical techniques for searching potential-energy surfaces. The calculated closed shell hydroxylation pathways, involving ^1S oxygen atoms, correspond to a concerted "attachment–rearrangement" mechanism, rather than to direct insertion of the oxygen. This mechanism has a characteristic barrier height of ~2 kcal/mol and does not involve ionic intermediates, thus implying retention of configuration. Triplet hydroxylation pathways, with ^3P oxygen atoms, were found to proceed via a two-step "abstraction–recombination" mechanism, the first step involving the formation of radical intermediates, with ~sevenfold higher barriers than for closed-shell hydroxylation. The closed shell epoxidation pathway for ethylene has a barrier of 1.4 kcal/mol and is concerted, implying retention of configuration, while the triplet epoxidation proceeds in two steps, the first having a barrier of 16 kcal/mol and leading to an open biradical oxygen adduct, implying loss of configuration. Based on these results, experiments are proposed to further elucidate P450 epoxidation mechanisms.

Introduction

The cytochrome P450's are a class of heme proteins involved in a wide variety of metabolic transformations[1] whose primary function is the solubilization of exogenous compounds, thereby facilitating excretion of the latter as metabolic products. It is now recognized that this same metabolism transforms a broad spectrum of relatively innocuous compounds into products with potent toxic and carcinogenic activity.[2] Because of the variety of possible substrates, this harmful, activating aspect of P450 metabolism assumes increasing importance as commerical products and by-products proliferate. Some of these are meant to be ingested and some not, but all must be regarded as potentially finding their way into the metabolic systems of higher organisms.

The diverse reactions comprising P450 metabolism seem to have a unifying characteristic. It has been well established that a single pass through the enzyme results in the formation of new covalent bonds in the substrate molecule, with incorporation of one atom of oxygen. This process either leads directly to stable products, such as alcohols and epoxides, or to reactive intermediates which go on to form the ultimate metabolic products.

In the present study attention has been focused on the P450 metabolism of hydrocarbons. In the context of polycyclic aromatic hydrocarbons and their activation to carcinogenic potency, the importance of P450 metabolism and the overall character of substrate transformations have been convincingly demonstrated.[2-6] Transformations of other types of hydrocarbons and the hydrocarbon portions of more complex molecules, e.g., fatty acids, have been studied by using P450 preparations[7,8] and model iron–porphine systems.[9]

The P450-mediated metabolism of hydrocarbons may be summarized in terms of two characteristic reaction types: "hydroxylations", in which C—H bonds are converted to C—O—H linkages, and epoxidations, which convert C=C bonds to oxirane rings. The precise nature of the active oxygen species in P450 and model iron–porphine reaction cycles is uncertain at present, although consensus favors an "oxenoid" model[8-10,13-15] in which a single oxygen is bound to the heme iron and reacts with substrates as something equivalent to a neutral oxygen atom, or oxene. The notion that this active oxygen species is "electrophilic" achieved prominence early,[18] and a formal analogy with the chemistry of peracids, such as trifluoroperacetic acid and other oxygenating agents, as well as with carbene and nitrene chemistry, has been noted often.[10-13] However, recent studies of P450-mediated epoxidations,[14,15] as well as of epoxidations catalyzed by other types of monooxygenase systems with similar function,[16,17] indicate that these analogies should not be carried too far and that the enzymatic active oxygen species is not electrophilic in the conventional sense. The calculated electronic structures[13] of chromyl chloride and a model ferryl (Fe–O) porphyrin complex feature low-lying virtual molecular orbitals with significant oxygen atom participation. This suggests that the active oxygen of the oxenoid model could function as an electrophilic center in the "overlap control" sense,[13] i.e., with respect to incipient covalent interactions with neutral substrates.

Detailed mechanistic interpretations of P450 hydrocarbon metabolism are complicated, since neither the mode of substrate binding (steric factors) nor the intrinsic nature of the reactions, i.e., free radical or other, has been resolved at present. In such a situation, the potential contribution of a reliable theoretical model is significant. If the characteristics of a number of candidate mechanisms in model systems can be elucidated and related to experimentally observable products and parameters, it might then

(1) J. R. Gillette, *Adv. Pharmacol.*, **4**, 219 (1966).
(2) W. Levin, A. W. Wood, A. Y. H. Lu, D. Ryan, S. West, A. H. Conney, D. R. Thakker, H. Yagi, and D. M. Jerina in "Drug Metabolism Concepts,", D. M. Jerina, Ed., ACS Symposium Series No. 44, American Chemical Society, Washington, D.C., 1977, p 99.
(3) J. W. De Pierre and L. Ernster, *Biochim. Biophys. Acta*, **473**, 149 (1978).
(4) D. M. Jerina and J. W. Daly, *Science*, **185**, 573 (1974).
(5) A. Borgen, H. Darvey, N. Castagnoli, T. T. Crocker, R. E. Rasmussen, and I. Y. Wang, *J. Med. Chem.*, **16**, 502 (1973).
(6) E. Huberman, R. Mager, and L. Sachs, *Nature (London)*, **264**, 360 (1976).
(7) M. L. Das, S. Orrenius, and L. Ernster, *Eur. J. Biochem.*, **4**, 519 (1968).
(8) J. T. Groves, G. A. McClusky, R. E. White, and M. J. Coon, *Biochem. Biophys. Res. Commun.*, **81**, 154 (1978).
(9) J. T. Groves, T. E. Nemo, and R. S. Myers, *J. Am. Chem. Soc.*, **101**, 1032 (1979).
(10) G. A. Hamilton, *J. Am. Chem. Soc.*, **86**, 3391 (1964).
(11) V. Ulrich, *Angew. Chem., Int. Ed. Engl.* **11**, 704 (1972).
(12) G. A. Hamilton in "Molecular Mechanisms of Oxygen Activation", O. Hayaishi, Ed., Academic Press, New York, 1974, p 405.
(13) G. H. Loew, L. M. Hjelmeland, and R. F. Kirchner, *Int. J. Quantum Chem., Quantum Biol. Symp.*, **4**, 225 (1977).
(14) R. P. Hanzlik, G. O. Shearer, A. Hamburg, and T. Gillesse, *Biochem. Pharmacol.*, **27**, 1435 (1978).
(15) R. P. Hanzlik and G. O. Shearer, *Biochem. Pharmacol.*, **27**, 1441 (1978).
(16) S. W. May, R. D. Schwartz, B. J. Abbott, and O. R. Zaborsky, *Biochim. Biophys. Acta*, **403**, 245 (1975).
(17) S. W. May, S. L. Gordon, and M. S. Steltenkamp, *J. Am. Chem. Soc.*, **99**, 2017 (1977).

0002-7863/80/1502-5443$01.00/0

be possible to isolate the purely electronic components of the enzymatic problem and select the most appropriate mechanistic model. Clearly, if the electronic features of the enzymatic pathways could be established in this manner, their other key aspects, e.g., steric factors, might be more readily approached.

This initial study examines the simplest possible systems which could serve as models for P450 hydrocarbon metabolism. The oxene hypothesis is followed through use of a neutral oxygen atom as the active species. The basic assumptions for this simplification are that substrates can interact directly with the oxygen of the P450 active species and that this step essentially involves the delivery of an oxene to the substrate. Both assumptions are consistent with current thinking regarding the oxenoid model.[8,9,19] In this study, hydroxylations and epoxidations are modeled by using methane and ethylene as "substrates." Both molecules may conceivably be too small to bind effectively, and thus might not serve as substrates themselves. Nevertheless, the underlying chemistry of the C—H and C=C bonds in these species should be "transferable" in some degree to the oxygenation behavior of more complex hydrocarbons: terminal methyl groups are hydroxylated by microsomal preparations,[18] and isolated double bonds in many compounds are smoothly epoxidated.[9,18] Further work will extend to larger molecules.

No attempt is made to introduce possible substrate interactions with the catalytic site. Since P450 metabolism is directed toward fat-soluble substrates, we can infer that such sites are predominantly hydrophobic,[19] and that transformed substrates no longer bind effectively after attaining sufficient hydrophilic character. We therefore assume that, in the enzymatic situation, intermolecular forces modulating the underlying "gas-phase" reaction will not be of large magnitude, so that direct study of such reactions will be relevant.

The semiempirical MINDO/3 SCF LCAO–MO method[20] is used to generate the potential surfaces in this study. This formalism has proved to be effective in calculating accurate optimized geometries and heats of formation for a wide variety of compounds, and these are the features one looks for when considering theoretical reaction path studies.[21] We employ both a modified "reaction profile/reaction coordinate" approach and a rigorous analytical technique[21,22] for searching potential-energy surfaces; both techniques are outlined below.

Closed-shell (singlet) and open-shell (triplet) potential surfaces are examined for a number of reaction paths. The triplet surfaces model free-radical mechanisms, while those arising from closed-shell surfaces are concerted and do not involve ionic intermediates. The MINDO/3 results suggest significant intrinsic differences between the two types of mechanism, which may be of use in elucidating the enzymatic oxygenation reactions.

Methodology

Our reaction profile calculations employed an updated version of the original MINDO/3 program.[22] Analytical searches of MINDO/3 potential surfaces were implemented by using the FORTRAN programs SIGMA, FORCE, and OPTMO.[23] All calculations were performed on the CDC 7600 computer at Lawrence Berkeley Laboratory.

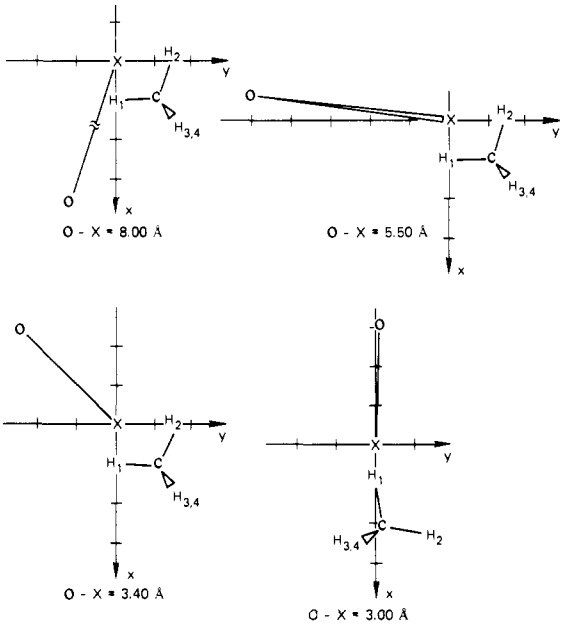

Figure 1. CH_4 + O closed shell, illustrating the dummy reaction coordinate technique. The dummy atom X is at the origin, and H_1 is fixed at x = 1.00 Å. All remaining internal coordinates are optimized. The x–y plane is shown, and the positive z axis comes out of the plane of the figure. Coordinate divisions are 1 Å.

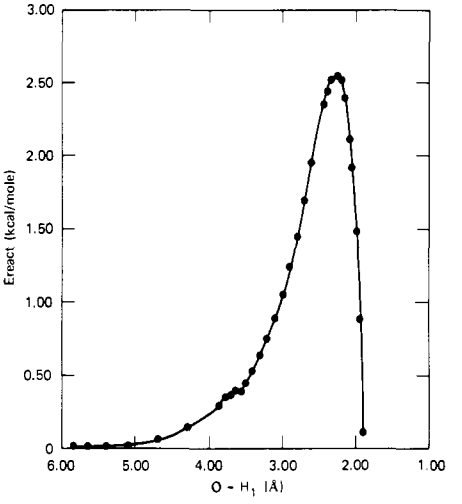

Figure 2. Partial reaction profile for the system of Figure 1, with the O–H_1 distance selected as reaction coordinate. The energy E_{react} is defined as the total energy for the given point minus the total energy of the isolated reactants.

Conventional reaction profile studies are subject to a certain arbitrary and intuitive element, which results from the selection of a "reaction coordinate" from the given set of internal molecular coordinates, i.e., bond lengths and angles and twist angles. The effectiveness of the resulting potential search will depend strongly on this choice, as well as on the coordinate system itself.[21,25]

In an attempt to minimize this intuitive, arbitrary character, we have introduced a method which might be termed the "dummy reaction coordinate" technique. Here, the distance between the oxygen and a dummy atom is chosen as "reaction coordinate", and this is fixed at a given value in the calculation of each point in the profile, while all remaining internal coordinates are allowed to optimize.

The use of the dummy coordinate is illustrated in Figure 1. A dummy atom was placed at the origin, and the overall geometry was defined so as to allow both oxygen and methane to reorient

(18) J. Daly in "Handbook of Experimental Pharmacology", Vol. XXVIII/2, B. B. Brodie and J. R. Gillette, Eds., Springer-Verlag, West Berlin, 1971, p 285.
(19) D. Dolphin, A. W. Addison, M. Cairns, R. K. Dinello, N. P. Farrell, B. R. James, D. R. Paulson, and C. Welborn, *Int. J. Quantum Chem.*, **16**, 311 (1979).
(20) R. C. Bingham, M. J. S. Dewar, and D. H. Lo, *J. Am. Chem. Soc.*, **97**, 1285 (1975).
(21) M. C. Flanigan, A. Komornicki, and J. W. McIver, Jr., in "Modern Theoretical Chemistry", Vol. 9, G. A. Segal, Ed., Plenum Press, New York, 1977, p 1.
(22) A Brown, M. J. S. Dewar, H. W. Kollmar, D. H. Lo, H. Metiu, P. J. Student, J. S. Wasson, and P. K. Weiner, *QCPE*, **11**, 279 (1975). Modifications were added at NRCC and in our laboratory.
(23) Written by A. Komornicki, who kindly made these programs available to us.
(24) J. W. McIver, Jr., and A. Komornicki, *J. Am. Chem. Soc.*, **94**, 2625 (1972).
(25) R. E. Stanton and J. W. McIver, Jr., *J. Am. Chem. Soc.*, **97**, 3632 (1975).

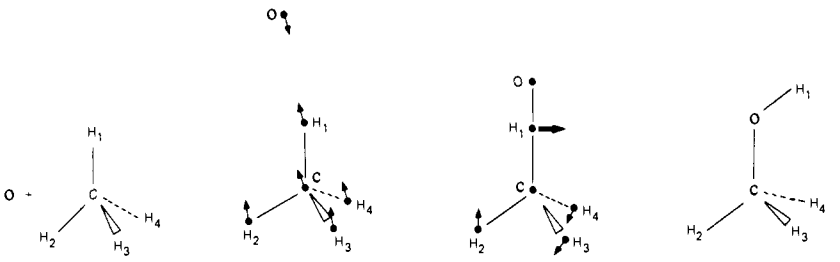

	Reactants	Transition State	"Intermediate" Saddle	Methanol
E (A.U.)	-18.006249	-18.002189	-18.094038	-18.293209
$O\text{-}H_1$ (Å)	7.028	2.262	0.979	0.952
C-O (Å)	8.019	3.364	2.132	1.340
$C\text{-}H_1$	1.102	1.104	1.153	1.898
$C\text{-}H_2$	1.102	1.102	1.101	1.119
$\angle$ $O\text{-}H_1\text{-}C$	- -	175.1	179.9	- -
$\angle$ $H_1\text{-}C\text{-}H_2$	109.4	109.4	104.9	- -
$\angle$ $H_1\text{-}C\text{-}H_3$	109.4	109.3	105.1	- -
$\angle$ $H_1\text{-}O\text{-}C$	- -	- -	- -	110.7
$\angle$ $O\text{-}C\text{-}H_2$	- -	- -	- -	107.9

Figure 3. Geometries and total energies for stationary point species along the $CH_4 + O(^1S) \rightarrow CH_3OH$ closed shell path. Geometries and total energies for stationary point species along the $CH_4 + O(^3P) \rightarrow CH_3 + OH$ triplet path.

on geometry optimization. Thus, the only constraint on the oxygen was that it remain on the surface of a sphere centered on the origin, with radius equal to the current value of the dummy coordinate. The figure shows clearly how one particular C–H bond becomes associated with the oxygen as the dummy coordinate is decreased. This establishes the character of the preferred reaction path in a more or less objective way, and it then becomes possible to choose the O–H distance as an approximation to the true reaction coordinate. With this as the horizontal axis, the usual type of reaction profile can be plotted. (See Figure 2 for the reaction profile of the system of Figure 1.)

An analytical search of a given potential surface affords a more rigorous way to determine reaction paths. The details of the procedure used here have been given by Flanigan et al.;[21] we now summarize its most important features. A simple reaction path on a given surface is characterized by three stationary points: two minima, corresponding to reactants and products, and a saddle point between them, corresponding to a transition state. In addition, a classical trajectory through the transition state gives the nuclear displacements necessary to convert reactants to products. The programs OPTMO and SIGMA, respectively, are used to locate minima and saddle points. The program FORCE is used to determine whether a given saddle point qualifies as a transition state: if the Cartesian force constant matrix corresponding to a given molecular geometry has one and only one negative eigenvalue, the species may be considered a transition state.[21,24,25] A Wilson F–G calculation[26] of the vibrational modes for a transition state will give the classical trajectory,[25] or true reaction coordinate, which is the mode corresponding to the single negative eigenvalue mentioned above. Displacement of the geometry in the manner indicated by the transition vibrational mode, followed by energy minimization (OPTMO) or gradient minimization (SIGMA), suffices to locate stationary points past the transition state. Thus, mechanistically important information is gained from the transition vibrational modes for the saddle points along this path.

Since the semiempirical methods employed were parametrized on the basis of heats of atomization at 298 K,[20-23] reaction enthalpies and barriers to reaction are obtained directly from calculated total energy differences. The reactant end of a path involves a separation of ~7 Å or more between the oxygen and the nearest hydrocarbon atom, while the product end is determined through total optimization from the last saddle point encountered.

Results

All stationary point species found by the analytical search method are characterized in Figures 3–8. In addition to geometry and total energy, displacement vectors indicating the nature of transition vibrational modes are given for all saddle-point species.

Although reaction profile calculations were also carried out for each of the reactions indicated, results are not given explicitly in these figures. This is because reaction profile results for reactants, products, and transition states are virtually identical with the analytical search results for closed-shell singlets, and quite similar for triplet paths. In the latter case, there are some discrepancies, because open-shell systems are treated differently in the two methods. While the SIGMA/FORCE/OPTMO package incorporates unrestricted calculation[23] of open-shell cases, the MINDO/3 program performs restricted calculations using the half-electron method.[27] The major effect of this difference in open-shell formalisms occurs in the calculated energies, which are compared in Table I.

In the closed-shell hydroxylations, the reaction profile method failed to give the intermediate saddle point species shown in Figures 3 and 7. In all cases, the maxima of reaction profile plots, such as that in Figure 2, gave species which were virtually at (closed shell) or very near (triplet) transition states. However, this method alone does not provide the required analytical verification of transition states. Thus, the general usefulness of reaction profile calculations in our work has been limited to the region up to and including the transition state, while detailed information of possible mechanistic import was derived from the analytical search method.

Important details regarding each reaction are summarized below. The possible significance of each of these is discussed in the next section.

(1) $CH_4 + O(^1S) \rightarrow CH_3OH$ Closed-Shell Path (Figure 3). In addition to a reactant-like transition state, an intermediate saddle point complex exists along the path. This species gives rise to two, nearly degenerate, negative force constant eigenvalues, indicating two virtually equivalent paths to the product. The vibrational mode

(26) E. B. Wilson, Jr., J. C. Decius, and P. C. Cross, "Molecular Vibrations", McGraw-Hill, New York, 1970, p 51.

(27) M. J. S. Dewar and N. Trinajstic, *J. Chem. Soc. A*, 1220 (1971).

(28) (a) These values were derived from the experimental heats of formation of the organic compounds[28b] and the atomic energies[28c] for ground-state ^3P and second excited state ^1S oxygen. (b) "JANAF Thermochemical Tables", Dow Chemical Co, Midland, Mich., 1965. (c) C. E. Moore, "Atomic Energy Levels", National Bureau of Standards, Washington, D.C., 1945.

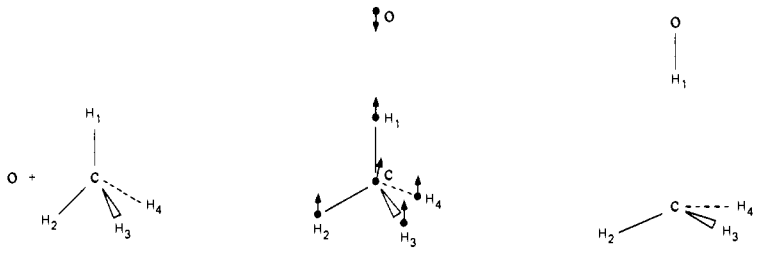

	Reactants	Transition State	Products
E (A.U.)	-18.091156	-18.080322	-18.121212
O-H_1 (Å)	8.101	1.704	0.947
C-H_1	1.102	1.114	3.081
C-H_2	1.102	1.102	1.092
∠ O-H_1-C	- -	175.9	179.5
∠ H_1-C-H_2	109.5	109.1	99.9
∠ H_1-C-H_3	109.5	109.6	117.0

Figure 4. Geometries and total energies for stationary point species along the $CH_4 + O(^3P) \rightarrow CH_3 + OH$ triplet path.

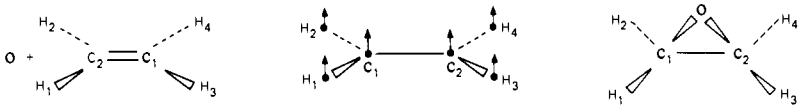

	Reactants	Transition State	Oxirane
E (A.U.)	-22.628669	-22.626497	-22.918752
C_1-O (Å)	8.027	3.197	1.389
C_1-C_2	1.314	1.315	1.447
C_1-H_1	1.100	1.100	1.114
∠ O-C_1-C_2	- -	77.8	
∠ H_1-C_1-C_2	124.6	124.6	123.9
∠ H_1-C_1-H_2	110.8	110.7	107.4

Figure 5. Geometries and total energies for stationary point species along the $H_2C{=}CH_2 + O(^1S) \rightarrow$ oxirane closed shell path.

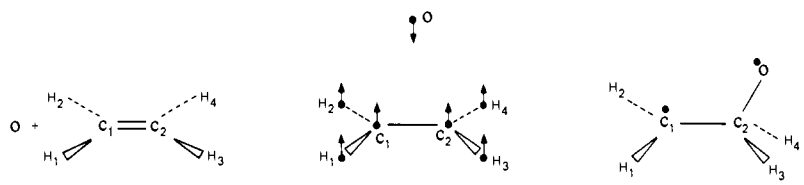

	Reactants	Transition State	Product
E (A.U.)	-22.713563	-22.707499	-22.830230
C_2-O (Å)	8.027	2.633	1.302
C_1-C_2	1.314	1.317	1.457
C_1-H_1	1.100	1.100	1.097
C_2-H_3	1.100	1.100	1.138
∠ O-C_2-C_1	- -	75.5	104.5
∠ H_1-C_1-C_2	124.6	124.7	122.9
∠ H_1-C_1-H_2	110.8	110.6	112.6
∠ H_3-C_2-C_1	124.6	124.7	110.9

Figure 6. Geometries and total energies for stationary point species along the $H_2C{=}CH_2 + O(^3P) \rightarrow H_2CC(O)H_2$ triplet path.

for only one of these is shown; the other is nearly identical, except that the direction of H_1 displacement is up out of the plane of the figure. A true hydrogen abstraction to form OH^- and CH_3^+ is not indicated by these results. Instead, the intermediate saddle point species has significant partial negative charge at the oxygen (−0.58) and partial positive charge at the carbon (+0.29). These charges may be compared with O(−0.46) and C(+0.39) for methanol and O(0.00) and C(+0.03) for the reactants. In the transition state, the partial charges are essentially those of the reactants.

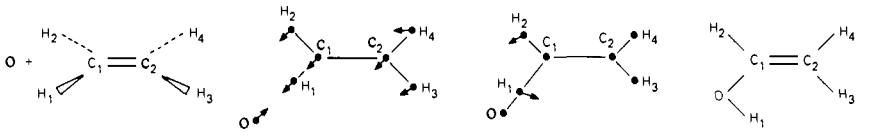

	Reactants	Transition State	"Intermediate" Saddle	Vinyl Alcohol
E (A.U.)	-22.628668	-22.625082	-22.723386	-22.933624
$O\text{-}H_1$ (Å)	7.616	2.298	0.973	0.952
$C_1\text{-}O$	8.716	3.399	2.130	1.321
$C_1\text{-}H_1$	1.100	1.102	1.156	1.907
$C_1\text{-}H_2$	1.100	1.100	1.100	1.117
$C_1\text{-}C_2$	1.314	1.314	1.301	1.328
$C_2\text{-}H_3$	1.100	1.099	1.095	1.096
$\angle$ $O\text{-}H_1\text{-}C_1$	- -	178.6	179.1	- -
$\angle$ $H_1\text{-}C_1\text{-}C_2$	124.6	- -	- -	- -
$\angle$ $H_1\text{-}C_1\text{-}H_2$	110.8	110.6	105.0	- -
$\angle$ $H_3\text{-}C_2\text{-}C_1$	124.6	124.9	127.6	121.7
$\angle$ $O\text{-}C_1\text{-}H_2$	- -	- -	- -	107.2

Figure 7. Geometries and total energies for stationary point species along the $H_2C{=}CH_2 + O(^1S) \rightarrow$ vinyl alcohol closed shell path.

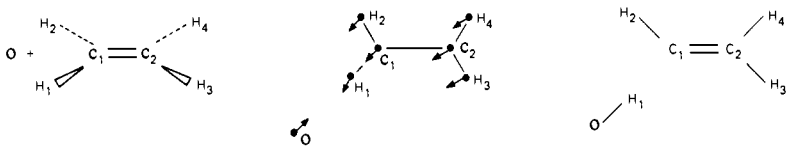

	Reactants	Transition State	Products
E (A.U.)	-22.713563	-22.703948	-22.747974
$O\text{-}H_1$ (Å)	8.152	1.750	0.949
$C_1\text{-}O$	8.027	2.859	3.233
$C_1\text{-}H_1$	1.100	1.109	2.284
$C_1\text{-}C_2$	1.314	1.313	1.292
$C_2\text{-}H_3$	1.100	1.100	1.105
$\angle$ $O\text{-}H_1\text{-}C_1$	- -	177.3	178.4
$\angle$ $H_1\text{-}C_1\text{-}C_2$	124.6	- -	- -
$\angle$ $H_1\text{-}C_1\text{-}H_2$	110.8	110.4	98.3
$\angle$ $H_3\text{-}C_2\text{-}C_1$	124.6	124.2	124.8

Figure 8. Geometries and total energies for stationary point species along the $H_2C{=}CH_2 + O(^3P) \rightarrow H_2C{=}CH + OH$ triplet path.

Table I. Calculated Enthalpies for Oxene + CH_4,$H_2C{=}CH_2$ Reactions

	$\Delta H^{\ddagger}$, kcal/mol			ΔH reaction, kcal/mol			
reaction[a]	cl shell	unrestricted	$^1/_2$ electron	exptl[21]	cl shell	unrestricted	$^1/_2$ electron
(1) $CH_4 + O \rightarrow CH_3OH$	2.6			−186.4	−180.1		
(2) $CH_4 + O \rightarrow CH_3 + OH$		6.8	15.8	+2.6		−18.9 (−19.4)[b]	−13.2 (+6.1)[b]
(3) $H_2C{=}CH_2 + O \rightarrow$ oxirane	1.4			−181.2	−182.0		
(4) $H_2C{=}CH_2 + O \rightarrow H_2CO(O)H_2$		3.8	16.3			−73.2	−65.1
(5) $H_2C{=}CH_2 + O \rightarrow$ vinyl alcohol	2.2				−191.4		
(6) $H_2C{=}CH_2 + O \rightarrow H_2C{=}CH + OH$		6.0	18.0	−2.9		−21.6 (−23.4)[b]	−14.1 (−9.7)[b]

[a] The odd-numbered reactions involve $O(^1S)$, while the even-numbered involve $O(^3P)$. [b] Values in parentheses are for completely isolated radicals as products.

(2) $CH_4 + O(^3P) \rightarrow CH_3 + OH$ Triplet Path (Figure 4). The results here indicate a straightforward hydrogen atom abstraction, with no stationary points between the transition state and product minimum.

(3) $H_2C{=}CH_2 + O(^1S) \rightarrow$ Oxirane Closed Shell (Figure 5). This reaction has a symmetrical transition state, which leads directly to the symmetrical oxirane product.

(4) $H_2C{=}CH_2 + O(^3P) \rightarrow H_2C(O)CH_2$ Triplet Path (Figure 6). This path also goes through a symmetrical transition state, which, however, leads to an unsymmetrical diradical product. The unrestricted calculation indicates nearly unit spin density on both C_1 and O.

(5) $H_2C{=}CH_2 + O(^1S) \rightarrow$ Vinyl Alcohol Closed Shell (Figure 7). As in (1) above, besides the transition state there is an intermediate saddle point species with two negative force constant eigenvalues of similar magnitude and vibrational modes along the path. Again, a true H abstraction with formation of OH^- and $H_2C{=}CH^+$ is not indicated.

(6) $H_2C{=}CH_2 + O(^3P) \rightarrow H_2C{=}CH + OH$ Triplet Path (Figure 8). The overall results are similar to those of (2) above.

They indicate a straightforward hydrogen atom abstraction.

The energetics of all the indicated reactions are summarized in Table I. Note that $\Delta H^{\ddagger}$ for all the triplet paths is higher than that of the corresponding closed-shell reactions, and that the closed-shell paths are highly exothermic. Also note that, where experimental results are available for the triplet paths, the half-electron formalism gives better agreement than the unrestricted calculation. This might have been anticipated, since the former method was used in the original parametrization of MINDO/3.[20] Therefore, we can assume that all the half-electron results given in Table I are to be preferred over their unrestricted counterparts.

Discussion

The large negative enthalpies of reaction for closed-shell paths are reproduced quite well by MINDO/3, while the calculated values for triplet paths are too exothermic, with a single exception. (See Table I.) The calculated barriers to reaction, $\Delta H^{\ddagger}$, are higher for the triplet paths. Experimental verification for this qualitative result is not available, however, since there does not yet appear to be a well-defined trend in gas-phase activation energies for reactions of atomic oxygen, in different electronic states, with various hydrocarbons.[29,30]

It should be pointed out that MINDO/3 heats of formation for some of the individual species, e.g., methane, ethylene, and oxirane, deviate significantly from the corresponding experimental values.[20] Yet, the results in Table I indicate that these individual errors tend to cancel when differences are taken. On the other hand, optimized geometries for the above-named species are in excellent agreement with experimental values.[20] Hence, we expect that a good degree of confidence may be assigned to energy differences (Table I) and geometries pertaining to transition states.

The performance of MINDO/3 with respect to the transition state for the $CH_4 + O$ triplet surface may be gauged by direct comparison with a recent ab initio study of the same system,[31] which used configuration interaction with an extended basis set, including polarization functions. The ab initio transition state is qualitatively very similar to that in Figure 4; however, the bond lengths in the former corresponding to $O-H_1$ and $C-H_1$ are respectively 1.25 and 1.32 Å, indicating that the transition-state geometry is midway between that of the reactants and products. This is expected on the basis of the Hammond postulate,[32] since the actual reaction is almost energetically balanced (Table I). The MINDO/3 geometry also follows the Hammond postulate: there is more resemblance to the reactants, since the MINDO/3 surface makes the overall reaction slightly exothermic. The uncorrected[31] ab initio barrier to reaction is 14.2 kcal/mol, to which the half-electron MINDO/3 value (Table I) compares favorably. Finally, both calculations agree as to the overall character of the free-radical mechanism, which involves hydrogen abstraction.

The MINDO/3 oxene model for hydrocarbon oxygenation thus far obtained has the following general features. Hydoxylations, closed shell and free radical, do not involve direct insertion of the oxygen. Instead, the closed-shell mechanism is best characterized as an "attachment–rearrangement" and is apparently concerted, thus implying retention of configuration. The triplet mechanism involves hydrogen abstraction to form hydroxyl and hydrocarbon radical intermediates which subsequently recombine, thus implying loss of configuration in the absence of steric constraints.

Both epoxidation mechanisms involve a symmetrical transition state with ethylene. One may easily infer that this will be the case for any symmetrically substituted alkene, and that the converse will hold for unsymmetrical alkenes. We have, in fact, obtained an unsymmetrical transition state in preliminary closed-shell results for propene and oxygen. The closed-shell epoxidation is concerted, implying retention of configuration about the C–C bond. The triplet mechanism, on the other hand, leads to an open biradical intermediate (Figure 6) which must "recombine" to close the oxirane ring. This implies loss of configuration about the C–C bond, if internal rotation in the intermediate is not hindered by steric constraints.

One of the more surprising implications of our results is that a closed-shell mechanism for hydroxylation need not involve the formation of formal carbocation and OH^- intermediates and could proceed with retention of configuration, which is consistent with a large body of experimental data on enzymatic hydroxylations.[18] Thus, such a mechanism is viable and, for the present, should be considered on an equal footing with free-radical mechanisms. Objections to a closed-shell mechanism[8,19] have hitherto been based on the assumption that formal carbocations must be involved, which would then imply the skeletal rearrangements and loss of configuration characteristic of fully ionic mechanisms.

At this initial stage, it is not yet possible to make any firm statements regarding the order of reactivity to be expected from a concerted closed-shell mechanism. The present results indicate only that vinyl and methane C–H bonds are equally reactive toward closed-shell hydroxylation. It is tempting to speculate that, since positive charge is built up on the carbon in these simple cases (see Results, above), the reactivities at various carbon centers in more complex molecules might follow the same order as do carbocation stabilities. However, it will not be possible to reach solid conclusions along these lines until studies of more complex hydrocarbons have been completed.

Further comparison of properties intrinsic to the closed-shell and radical mechanisms indicates that they qualitatively parallel one another, apart from the configuration retention aspect already noted. For example, the ethylene results in Table I show that calculated barriers for expoxidation are lower than for hydroxylation in both mechanisms. This qualitative characteristic of the MINDO/3 surfaces agrees with the general preference of P450,[14,15] model iron–porphine systems,[9] and a bacterial monooxygenase system[17] for epoxidation over hydroxylation in compounds which can serve as substrates for both reactions. Finally, since the order of reactivity for closed-shell hydroxylations is not yet established, selectivity alone will not presently aid in choosing between the closed-shell and radical mechanisms.

A radical abstraction–recombination mechanism for P450 hydroxylation, based on the oxene model, is currently gaining support.[8,19] To account for the retention of configuration which appears to be a major feature of P450 hydroxylations, it is necessary to postulate steric constraints, e.g., an enzyme–substrate "cage"[8] or something equivalent, as an adjunct to a radical mechanism. The recent work of Groves et al.[8] on in vitro P450 hydroxylation of deuterated norbornane actually indicates that not all such hydroxylations need proceed with complete retention of configuration. The vast majority of available data, however, indicate that, if a free-radical mechanism is indeed operative, steric constraints are masking the loss of configuration which is an intrinsic feature of this pathway.

It is likely that P450 epoxidations will provide a better test of the proposed mechanism: the closed-shell mechanism is concerted, while the radical mechanism allows for loss of configuration by rotation about the C–C bond in the biradical intermediate. As far as we could ascertain, substrates designed to test this feature have not been looked at, since the overwhelming emphasis in P450 literature has been on cyclic compounds with carcinogenic or other biological activity.[33] A study of the general type we suggest has been performed, but with the monooxygenase system of *Pseudomonas oleovorans*,[17] which apparently does not involve cytochrome P450 enzymes. The authors found that epoxidation of *trans,trans*-1,8-dideuterio-1,7-octadiene proceeds with 70% *inversion* of configuration. These authors conclude that a simple "oxenoid" mechanism is not consistent with their results. However, the present work now indicates that a straightforward radical oxene epoxidation, with an unsymmetrically substituted double bond, would qualitatively account for the experimental results quite well.

(29) W. B. DeMore and O. F. Raper, *J. Chem. Phys.*, **46**, 2500 (1967).
(30) W. S. Nip, D. L. Singleton, and R. J. Cvetanovic, *Can. J. Chem.*, **57**, 949 (1979).
(31) S. P. Walch and T. H. Dunning, Jr., *J. Chem. Phys.*, in press.
(32) G. S. Hammond, *J. Am. Chem. Soc.*, **77**, 334 (1955).
(33) R. C. Garner in "Progress in Drug Metabolism", Vol. 1, J. W. Bridges and L. F. Chasseaud, Eds., Wiley-Interscience, New York, 1976, p 77.

Our suggestion is that an analogous experimental study, with the cytochrome P450 enzymes, be carried out.

The possible problems involved are brought out in a recent study using a model iron–porphine system, with iodosylbenzene as the oxygen source.[9] Epoxidation of *cis*-stilbene proceeds with 82% yield to give the cis epoxide, while *trans*-stilbene is almost completely unreactive. The drastic difference in reactivity is easily ascribable to steric constraints at the catalytic site,[9] which would also hinder internal rotation in a biradical intermediate if a radical mechanism is involved.

The strategy we suggest is as follows: Steric factors might be minimized if one could find an olefinic substrate whose cis and trans isomers show similar reactivity toward P450 epoxidation. If one could also reasonably expect that internal rotation in a possible biradical intermediate would not be drastically hindered, such a substrate would provide an acceptable probe of mechanism.

We are currently engaged in further exploration of some of the questions raised in the present study, through modeling the hydroxylation and epoxidation of propene by oxene. Using the methods outlined here, in conjunction with theoretical evaluation of vibrational partition functions and thermodynamic activation parameters,[21] we hope to more rigorously address the reactivity–selectivity problem mentioned above. The allyl and vinyl carbons of propene, for example, represent extremes of reactivity in both ionic and radical reactions. Also, the unsymmetrical environment about the double bond is expected to affect the epoxidation mechanisms, in that two biradical intermediates are possible with, we expect, unequal stabilities.

Acknowledgments. The authors wish to thank Dr. Andrew Komornicki for making his programs, SIGMA, FORCE, and OPTMO, available to them, and James Ferrell and Dr. Stanley Burt for many helpful discussions. They also gratefully acknowledge the financial support provided for this work by National Institute of General Medicine Grant GM27943-01 and National Cancer Institute Contract NCI 1-CP75928.

Vibrational Optical Activity in Para-Substituted 1-Methylcyclohex-1-enes

Prasad L. Polavarapu, Max Diem, and Laurence A. Nafie*[1]

Contribution from the Department of Chemistry, Syracuse University, Syracuse, New York 13210. *Received January 10, 1980*

Abstract: We report Raman optical activity (ROA) between 1300 and 1500 cm^{-1} and vibrational circular dichroism (VCD) between 2800 and 3000 cm^{-1} for (+)-*p*-menth-1-ene and (+)-*p*-menth-1-en-9-ol. The ROA data were obtained from a newly constructed spectrometer, the details of which are described. In addition, we have measured the VCD of (+)-limonene in the CH stretching region which complements the ROA spectrum of (−)-limonene available in the literature. All three molecules have the same ring structure and differ only at the para position. Since the vibrational optical activity (VOA) of these molecules in the regions selected is strongly similar we conclude that, contrary to general expectation, degenerate methyl modes do not make dominant contributions here. Instead, ring methylene modes are implicated as the major source of VOA intensity. It is encouraging that both VCD and ROA reinforce this spectral interpretation and therefore each other. This study of VOA is the first in which new spectral data for both VCD and ROA are presented.

I. Introduction

Current research in vibrational optical activity (VOA) has revealed considerable potential for exploring molecular stereochemistry.[2-5] Recently, correlations between observed Raman optical activity (ROA) and stereochemical details in two series of related molecules have been reported.[6,7] Similar correlations have been noted in the vibrational circular dichroism (VCD) of amino acids,[8,9] peptides,[10] sugars,[11] and several organic molecules.[12-15] In this paper we present VOA spectra for three closely related cyclohexene molecules which differ only by their substituent at the para position. This study is unique in that new experimental data for *both* VCD and ROA are presented. The combined results are then used to interpret the stereochemical origin of the major spectral features. Our approach here is to study VCD and ROA in closely related spectral regions which permits reinforcing interpretations of the data. This circumvents the general problem of lack of overlap between the usual spectral regions of VCD and ROA, although improvements in instrumentation[16-18] in the near future should reduce this problem by

(1) Alfred P. Sloan Foundation Fellow.
(2) L. D. Barron, *Adv. Infrared Raman Spectrosc.*, (1978).
(3) L. D. Baron in "Optical Activity and Chiral Discrimination", S. F. Mason, Ed., D. Reidel Dordrecht, Holland, 1979, p 219.
(4) P. J. Stephens and R. Clark in ref 3, p 263.
(5) L. A. Nafie and M. Diem, *Acc. Chem. Res.*, **12**, 296 (1979).
(6) L. D. Barron and B. P. Clark, *J. Chem. Soc., Perkin Trans. 2*, 1164 (1979).
(7) L. D. Barron and B. P. Clark, *J. Chem. Soc., Perkin Trans. 2*, 1171 (1979).
(8) M. Diem, P. J. Gotkin, J. M. Kupfer, A. P. Tindall, and L. A. Nafie, *J. Am. Chem. Soc.*, **99**, 8103 (1977).
(9) M. Diem, E. Photos, H. Khouri, and L. A. Nafie, *J. Am. Chem. Soc.*, **101**, 6829 (1979).
(10) M. Diem, P. J. Gotkin, J. M. Kupfer, and L. A. Nafie, *J. Am. Chem. Soc.*, **100**, 5644 (1978).
(11) C. Marcott, H. A. Havel, J. Overend, and A. Moscowitz, *J. Am. Chem. Soc.*, **100**, 7088 (1978).
(12) H. Sugeta, C. Marcott, T. R. Faulkner, J. Overend, and A. Moscowitz, *Chem. Phys. Lett.*, **40**, 397 (1976).
(13) T. A. Keiderling and P. J. Stephens, *J. Am. Chem. Soc.*, **99**, 8061 (1977).
(14) C. Marcott, C. C. Blackburn, T. R. Faulkner, A. Moscowitz, and J. Overend, *J. Am. Chem. Soc.*, **100**, 5262 (1978).
(15) T. A. Keidering and P. J. Stephens, *J. Am. Chem. Soc.*, **101**, 1396 (1979).
(16) L. A. Nafie, M. Diem, and D. W. Vidrine, *J. Am. Chem. Soc.*, **101**, 496 (1979).
(17) H. Boucher, T. R. Brocki, M. Moskovits, and B. Bosnich, *J. Am. Chem. Soc.*, **99**, 6870 (1977).

0002-7863/80/1502-5449$01.00/0